

Recent steps and perspectives on quasifission studies with the VAMOS variable-mode spectrometer at GANIL (France)

Manuel Caamaño^{1,*}, Daniel Fernández-Fernández^{1,**}, Diego Ramos², Antoine Lemasson², Maurycy Rejmund², Giorgia Mantovani^{1,3,4,***}, Christelle Schmitt⁵, Dieter Ackermann², Héctor Álvarez-Pol¹, Laurent Audouin⁶, Sayani Biswas^{2,****}, Michał Ciemała⁷, Emmanuel Clément², Dominique Durand⁸, Fanny Farget², Beatriz Fernández-Domínguez¹, John D. Frankland², Marc Olivier Frégeau^{2,†}, Daniel Galaviz⁹, Elisabet Galiana-Baldó^{1,9,‡}, Andreas Heinz¹⁰, Ana Isabel Henriques^{9,§}, Bertrand Jacquot², Beatriz Jurado¹¹, Yung Hee Kim^{2,¶}, Pierre Morfouace^{2,||}, Damian Ralet^{2,**}, Thomas Roger², Pamela Teubig⁹, and Igor Tsekhanovich¹¹

¹IGFAE – Universidade de Santiago de Compostela, E-15706 Santiago de Compostela, Spain

²GANIL, CNRS/IN2P3, CEA/DRF, Bd Henri Becquerel, 14076 Caen, France

³INFN, Laboratori Nazionali di Legnaro, IT-35020 Legnaro (Padova), Italy

⁴Università degli Studi di Padova, Padova, Italy

⁵Institut Pluridisciplinaire Hubert Curien, CNRS/IN2P3-UDS, 67037 Strasbourg Cedex 2, France

⁶IJC Lab, Université Paris-Saclay, CNRS/IN2P3, 91405 Orsay, France

⁷Institute of Nuclear Physics Polish Academy of Sciences, 31342 Kraków, Poland

⁸LPC Caen, Université de Caen Normandie, ENSICAEN, CNRS/IN2P3, Bd Maréchal Juin, 14050 Caen, France

⁹University of Lisbon – Faculdade de Ciências, Campo Grande, Lisbon, 1649-016, Portugal

¹⁰Department of Physics, Chalmers University of Technology, SE-41296 Göteborg, Sweden

¹¹LP2i Bordeaux, 19 Chemin du Solarium 33170 Gradignan, France

Abstract. The quasifission process is a close relative of fusion–fission. In both reaction channels, two nuclei collide to form a system that splits into two fragments. However, while fully equilibrated compound systems are formed during fusion–fission reactions, in quasifission, the system is out of equilibrium during the process. In this paper, we show that the experimental measurement of the atomic number of quasifission fragments reveals a strong even–odd staggering in the isotopic yields, which, in turn, can be used as a marker for nucleon dynamics. The measured data demonstrate the action of two distinct nucleon drift flows, which can be associated with the initial isospin equilibration and the subsequent mass drift.

1 Introduction

In a typical quasifission reaction (QF), two nuclei collide with a certain impact parameter that is translated into a continuous rotation of the quasi-system, which consists in the two nuclei precariously joined by their surfaces since the Coulomb repulsion prevents the complete fusion into an equilibrated compound system (CS). During the relatively short time they are together (comparable to the ro-

tation frequency), nucleons flow between them driven by the asymmetry component of the nuclear interaction and the surface tension, until they separate into two fragments. Since the process evolves out of equilibrium, the exit channel keeps some memory of the properties of the initial configuration such as the incident direction and the nature of the participants [1].

The study of QF is particularly interesting due to its connection to other reaction channels. Fusion can be drastically hindered by QF when the initial nuclei are of a significant size. Since nuclear fusion is currently one of the main strategies to form superheavy elements, a systematic understanding of QF reactions can help to find particular configurations that maximise the fusion probability [2]. The understanding of fission can also profit from QF studies. Since QF explores a similar potential energy surface, it may help to separate the effect of the fission barrier from the descend towards scission, and to better define the role of nuclear structure and particular shells along the path in the potential energy surface [3].

Besides these connections, QF offers a unique laboratory where different nucleon dynamics are at play. The

*e-mail: manuel.fresco@usc.es

**Current affiliation: Universidad Internacional de La Rioja, Logroño, Spain

***Current affiliation: Newcleo Ltd. Bologna, Italy

****Current affiliation: ISIS facility, STFC Rutherford Appleton Laboratory, Didcot OX11 0QX, United Kingdom

†Current affiliation: CEA DAM Île-de-France, Bruyères-le-Châtel, France

‡Current affiliation: ACPRO SLU, Barcelona, Spain

§Current affiliation: Facility for Rare Isotope Beams, Michigan State University, 640 South Shaw Lane, East Lansing, 48824, MI, USA

¶Current affiliation: Center for Exotic Nuclear Studies, Institute of Basic Science, Daejeon 34126, Republic of Korea

||Current affiliation: CEA, DAM, DIF, Arpajon, France

**Current affiliation: Mirion Technologies France, Lingolsheim, France

timescale of QF allows to study the diffusion and exchange of nucleons between the participants that impact the resulting equilibration, dissipation, and energy sharing of the final fragments [4].

In this work, we show the first experiment to directly measure the atomic number Z of fragments in QF reactions. The isotopic distribution of QF fragments yields shows a clear even–odd staggering that reflects the dynamics of the nucleons, including the dissipation mechanism, in the different stages of the process.

2 Measuring the onset of quasifission with VAMOS

A recent experiment focused on the study of high-energy fission was performed with the VAMOS variable-mode spectrometer at the GANIL facilities, in France [5, 6]. The experiment was based on collisions between a ^{238}U beam and a series of targets, which included ^{27}Al . This reaction channel has already been measured in a previous experiment, where signatures of slow QF were identified [7, 8]: a clear asymmetry in the mass–angle distribution (MAD), which leads to a wider distribution when compared to fission, and a higher angular anisotropy. In this respect, [7, 8] are used as a reference for the present data, which add the isotopic identification of the fragments.

2.1 Experimental setup

Since 2008, a series of fission experiments are being performed in VAMOS with modified versions of the same setup, intended to measure fission of systems produced in inelastic, transfer, and fusion reactions in inverse kinematics (see [9–12] among others).

In order to reconstruct binary reactions leading to fissioning systems, a set of ancillary detectors, typically stacks of silicon stripped detectors, measures the angle, energy loss, and energy of the target-like recoils. From them, the CS is identified and its excitation energy and centre of mass (c.m.) vector, determined [13].

After fission, any fragment emitted within the VAMOS acceptance is detected in the spectrometer. The magnetic rigidity, angle of emission, velocity, energy loss, and energy of the fragment are measured, from which its Z and mass number (A) after neutron evaporation are obtained. In most of the experiments, a gamma detector such as EXOGAM [14] or AGATA [15] is used to confirm the fragment identification. Occasionally, an additional second arm is placed to detect, in coincidence, the partner of the fragment detected in VAMOS [12].

In the case of the present iteration, a ^{238}U beam at 5.84 A MeV impinged on a $200\text{-}\mu\text{g}/\text{cm}^2$ ^{27}Al target to produce fusion reactions forming ^{265}Db with an excitation energy of 61.2 MeV. This CS may fission after evaporating a number of neutrons, and one of the fragments can be detected in VAMOS. In this case, the anti-coincidence with target-like recoils tags a fusion–fission channel instead of transfer- or inelastic-induced fission.¹

¹Granted, a detailed analysis eliminates contamination from transfer- and inelastic-induced reactions happening out of the acceptance of the

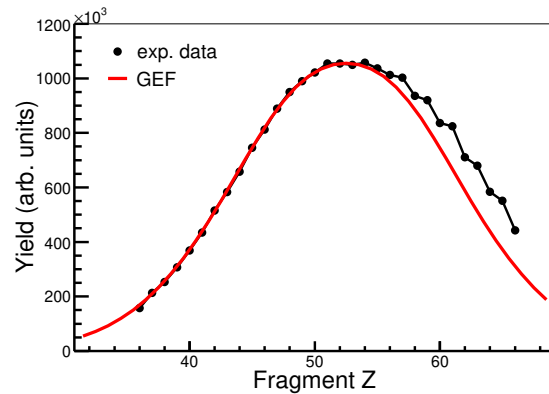


Figure 1. Black dots: Isotopic yield distribution of fragments produced in $^{238}\text{U}+^{27}\text{Al}$ collisions emitted between 45.6° and 60° in c.m. as measured with VAMOS. The error bars are smaller than the symbols. The red line shows the yield distribution predicted by the GEF code for fission of ^{265}Db with an excitation energy of 61.2 MeV and an average angular momentum of $\langle l \rangle = 14\hbar$.

The use of a magnetic spectrometer in inverse kinematics is not free of certain limitations. The angular coverage in c.m. is significantly reduced when compared to similar measurements where large area detectors can be used to cover most of the c.m. distribution. In the present case, the VAMOS data cover an angular window between 45.6° and 60° in c.m., while the isotopic identification includes fragments between $Z=34$ and $Z=66$, and post-neutron evaporation mass from $A=78$ to $A=170$, with resolutions of the order of 1%.

2.2 Fragment yields

Figure 1 shows the isotopic yield distribution of fragments produced in $^{238}\text{U}+^{27}\text{Al}$ measured with VAMOS. The data is compared to the predictions of the GEF code [17] for fission of ^{265}Db with an excitation energy of 61.2 MeV and an angular momentum of $\langle l \rangle = 14\hbar$. The yield distribution shows two distinct features: a clear asymmetry and a certain even–odd staggering towards heavier fragments.

The first feature is a direct consequence of the QF production: whereas the shape of the fission-yield distribution is independent on the emission angle, QF distributions result from the correlation between the probability of breaking up the system at a certain time, which defines an emission angle, and the mass drift that defines the size of the fragments. In our case, the excess observed in the heavy side of the distribution renders the distribution asymmetric because the light partners are emitted in the opposite angle in c.m., which is out of the acceptance window of this experiment (see Fig. 2).

target-like recoil detection set. Further details on the experimental setup and methods can be found in [16].

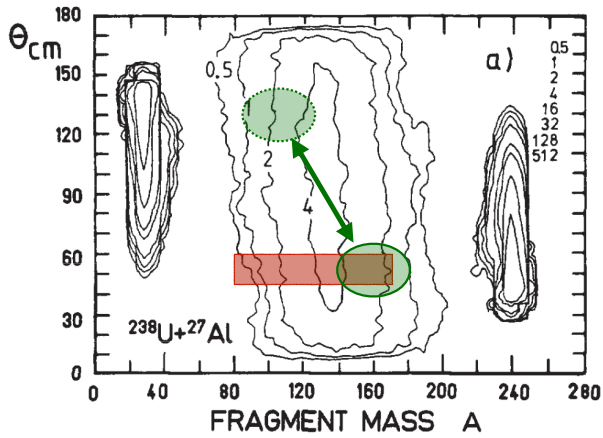


Figure 2. The figure shows the mass–angle distribution from $^{238}\text{U}+^{27}\text{Al}$ as reported in [8]. The red square corresponds to the angular acceptance and mass limits of the VAMOS data. The semi-transparent green ellipses circle the position of the yield excess of heavy fragments in the VAMOS data (solid contour) and that of the corresponding light partners (dashed contour).

2.3 Even–odd staggering in quasifission

The second feature of the fragment yields, the even–odd staggering in the distribution, is a well-known phenomenon in fission [18–20] that is strongly related to the generation of intrinsic energy along the process [21–23], and thus to dissipation effects and the timescale of fission [24]. However, the even–odd staggering is also known to disappear with increasing excitation energy. In our case, with 61.2 MeV of energy in the CS, a negligible even–odd staggering is expected from fusion–fission [22, 23].

In order to quantify the even–odd staggering, the amplitude δ can be defined as the proportion that the measured yields $Y_m(Z)$ deviate from an underlying smooth behaviour $Y_s(Z)$ as: $Y_m(Z) = Y_s(Z)[1 + (-1)^Z\delta]$. Figure 3 shows δ as a function of Z computed as described in [18].² The sensitivity of δ is limited by the underlying assumptions and, more importantly, by the statistical fluctuations of the measured data. In this case, measured values below $|\delta| < 0.01$ are compatible with no even–odd effect [25].

The amplitude of δ is statistically significant above $Z=57$, which is also the region where the measured yield deviates from the expected fission distribution as shown in Fig. 1, while it remains compatible with $\delta = 0$ in the rest of the distribution. It stands to reason then that the even–odd staggering is produced by the QF component of the measured yield distribution, making this one the first observation of even–odd staggering in QF reactions.

Also relevant is the negative sign of δ above $Z=57$. This implies a higher probability of producing odd- Z than even- Z heavy fragments. This is a remarkable observation considering that the initial participants are the odd- Z light ^{27}Al and the even- Z heavy ^{238}U . Somehow, the heavy

²This prescription computes an average amplitude in a moving window of four consecutive Z yields, hence the semi-integer result for the average Z . See [25] for more details and limitations of the method.

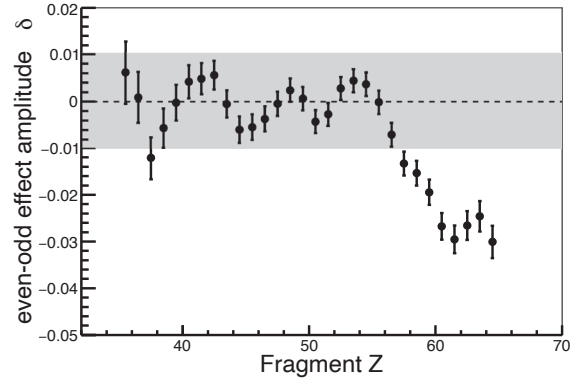


Figure 3. Local amplitude δ of the even–odd effect in isotopic yields as a function of the fragment Z . The shadowed area shows the limits of measured δ values statistically compatible with $\delta = 0$.

partner is able to transfer more than 30 protons to the light one while retaining an odd number of protons. In order to understand this, we should look into the expected nucleon flow and dynamics between both participants.

3 Mass and isospin equilibration in quasifission

Right after the reaction partners make contact, a series of exchanges tend to equilibrate the system. The first and faster stages correspond to the equilibration of the asymmetry between protons and neutrons, and the damping of the initial kinetic energy and angular momentum. These are fairly complete in few zs and possibly accomplished through a common mechanism of nucleon exchanges between the pre-fragments. After these quick exchanges, and for some 20 zs, the quasi-system experiences a mass drift that transports nucleons from the heavy partner to the light one towards mass symmetry. Interestingly, the behaviour and timescales of each of these equilibration mechanisms seem to be universal and independent on the entrance channel [4].

Following this picture, a fast equilibration of the neutron–proton asymmetry, defined as the difference between the fragments of a sort of normalised isospin $I(t) = (A_1 - 2Z_1)/A_1 - (A_2 - 2Z_2)/A_2$, can explain the negative sign of the measured δ . The degree of equilibration is tracked with respect to the initial $I(t = 0)$: $\delta I = |I(t)|/I(t = 0)$.³ Notice that, before making contact, $\delta I = 1$; total equilibration tends to $\delta I = 0$; and that the protons of each participant are initially paired except in ^{27}Al , where an unpaired proton is present.

In order to approach δI with few transfers and small changes in the mass, a possibility is moving one proton from ^{27}Al to ^{238}U and two neutron pairs in the opposite

³This is an approximation of the actual definition. A more strict version can be found in [4] (incidentally, notice the typo in the definition of I in page 3 of the same reference).

direction, resulting in ^{30}Mg and ^{235}Np , and $\delta I = 0.05$. Another option is the transfer of three neutron pairs to ^{27}Al , resulting in ^{33}Al and ^{232}U , and $\delta I = 0.03$.⁴ Therefore, the presence of the unpaired proton in the heavy partner can be interpreted as an experimental evidence of the nucleon exchanges that lead to the δI equilibration.

After the initial δI equilibration, the mass drift remains the primary equilibration process until the quasi-system splits. It can be proved that the transfer of protons from the heavy pre-fragment to the light one reduces δ [26], thus the fact that a measurable amplitude remains after the exchange of more than 30 protons is remarkable.

3.1 A note on the difference in the even–odd effect in fission and quasifission

Although the even–odd staggering is strongly related to the intrinsic excitation energy and its capacity for breaking nucleon pairs, it is important to note that the experimental link between δ and any property of the fission and QF process appears only if these unpaired nucleons move between the pre-fragments. In fission, this exchange is mostly governed by the level density of the pre-fragments and the temperature regime [27]. This can be demonstrated with the systematic observation of negative δ in heavy fragments of odd- Z CS [19]. However, in QF, the underlying mechanism of nucleon exchange is fundamentally different.

In the previous section, the generation of even–odd staggering in QF isotopic yields is understood as a consequence of back and forth transfers between the reaction partners, which, in turn, are driven by the asymmetry term of the nuclear force in the few zs after contact and, afterwards, by the surface tension trying to reach mass symmetry. The latter transfers nucleons from the heavy to the light pre-fragment, that is, in the opposite direction of that of fission, where the difference in temperature pushes energy and nucleon transfer from the light to the heavy pre-fragment, and also shapes the behaviour of δ [28].⁵

The difference in the mechanisms for the generation of δ in fission and QF also puts constraints on the use in QF of phenomenological relations between δ and the total intrinsic energy based on fission data [22, 29].

4 Estimation of the QF and fission contributions in the measured yields

In previous sections, the discussion and conclusions from the observation of the even–odd effect in QF are done in a qualitative way. The amplitude δ is computed with respect to the total measured yield distribution, which is the sum of fission and QF events. Therefore, the δ amplitudes displayed in Fig. 3 are smaller than the actual effect produced by QF reactions.

⁴Other combinations, including the option of breaking pairs to have more unpaired protons, either result in higher δI , need more exchanges, or change significantly the masses of the participants.

⁵However, a certain influence of the temperature difference between the pre-fragments cannot be completely ruled out; particularly, when the sticking time is long, the quasi-system is close to the mass symmetry, and the strength of the mass equilibration weakens.

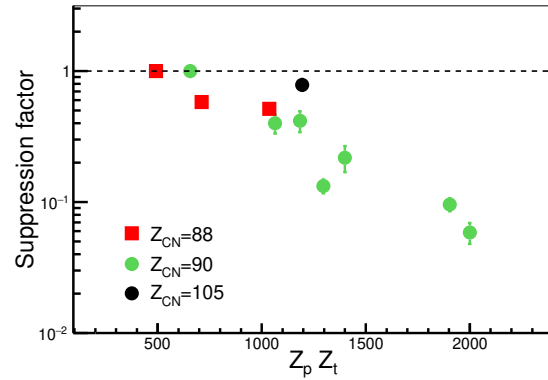


Figure 4. Suppression factor of complete fusion as a function of the product of the atomic numbers of projectile Z_p and target Z_t . Green dots correspond to reactions forming ^{220}Th [31]. Red squares correspond to reactions forming ^{216}Ra [32]. The black dot is the estimation from the present work corresponding to ^{265}Db . See [30, 31] for a detailed description of the suppression factor.

To have a more quantitative discussion, the fission yield distribution should be subtracted from the total. But an estimation of the fraction of fission and QF is not straightforward. Usually, the presence of QF in fusion–fission reactions is signalled by any correlation in the MAD, a pronounced anisotropy in the angular distribution, and a mass distribution wider than expected in fission reactions. From these signatures, Tōke et al. estimate a 70% of QF in $^{238}\text{U}+^{27}\text{Al}$ collisions [8].

In a recent study, direct measurements of fusion probabilities in a series of channels are combined with previous data to reveal a systematic behaviour of the suppression factor of compound nucleus formation that seems to fall exponentially with the product of the atomic numbers of the participants $Z_p Z_t$ [30, 31]. Figure 4 shows these results, which correspond to ^{220}Th CS, together with data from [32] that correspond to ^{216}Ra . The overall exponential trend suggests a suppression factor between 0.3 and 0.5 for the $Z_p Z_t = 1196$ of the $^{238}\text{U}+^{27}\text{Al}$ collisions, thus between 50% and 70% of QF.

However, the measured properties of the $^{238}\text{U}+^{27}\text{Al}$ data suggest the suppression factor might be quite different. The behaviour of a set of observables show strong variations as a function of Z , with values that are consistent with fusion–fission reactions below $Z \sim 56$ but unexpected above. The first observable, as already presented, is the even–odd effect: below $Z \sim 56$, the amplitude δ is compatible with no effect, which is consistent with fission at high energy [33]; however, the presence of a visible even–odd staggering for heavier fragments is completely unexpected. Figure 5 shows the evolution of two other observables: the standard deviation of the post-evaporation mass distributions for each fragment Z , σ_A ; and the normalised slope of the angular distribution for each fragment Z in the angular region of the present work, computed as

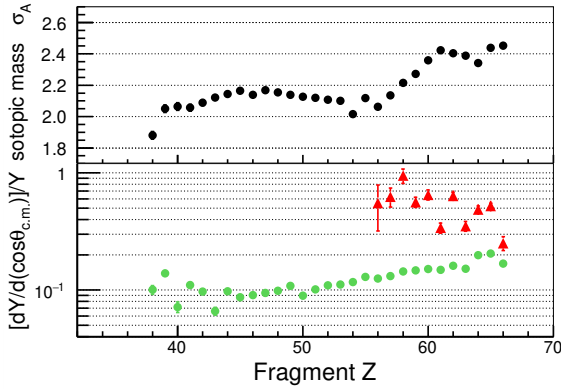


Figure 5. Top panel: Standard deviation of the post-evaporation mass distributions for each fragment Z , σ_A . Bottom panel: Slope of the angular distribution normalised to the yield Y in the angular region of the present work, $[dY/d\cos\theta_{c.m.}]/Y$ (green dots); normalised slope of the difference between the angular distribution of complementary fragments (red triangles).

$[dY/d\cos\theta_{c.m.}]/Y$, where Y is the yield.⁶ In high-energy fusion-fission, a smooth σ_A is expected due to post scission neutron evaporation and the absence of strong shell effects, however, the measured σ_A shows a clear discontinuity around $Z\sim 56$, where it jumps from a roughly constant value of $\sigma_A(Z)\sim 2.1$ to $\sigma_A(Z)\sim 2.4$. In a similar way, the angular distribution from fusion-fission is expected to have a very mild, if any, dependence on the fragment size. But, most importantly, complementary fragments with atomic numbers Z and $(105-Z)$ should have the same angular distribution. However, the slope of the angular distribution below $Z\sim 56$ fluctuates around a constant value while, for heavier fragments, the slope increases until doubling its value. Figure 5 also shows the slope of the difference between the angular distribution of complementary fragments. If these were produced in an equilibrated CS, this slope would be compatible with 0 but the results are several times higher than those expected in fission.

Besides these indications, the width of the fragment distribution can be also used to determine the degree of contribution of complete fusion-fission. In Ref. [30], a remarkable conclusion is put forward: of the common indicators of QF (MAD, mass distribution width, and angular anisotropy), "[t]he change in [mass width] is the only signature of compound nucleus suppression evident in the fission characteristics at small $Z_p Z_t$ ". A reasonable expectation of the fragment Z distribution can be obtained from the GEF code. Figure 1 shows the calculated fragment Z distribution for fission of ^{265}Db with 61.2 MeV of excitation energy and a mean angular momentum of $14\hbar$. The GEF distribution has an almost identical shape as that of the measured data up to $Z\sim 52$.⁷ Figure 6 shows the dif-

⁶This is an alternative way of addressing the angular anisotropy. In this work, the small angular region is not particularly sensitive for a precise determination of the relevant quantum numbers.

⁷The GEF code tends to underestimate the widths of Z or A distributions from high-energy fission when compared to measured data. They can be taken as factual lower limits (see [16, 34] for instance).

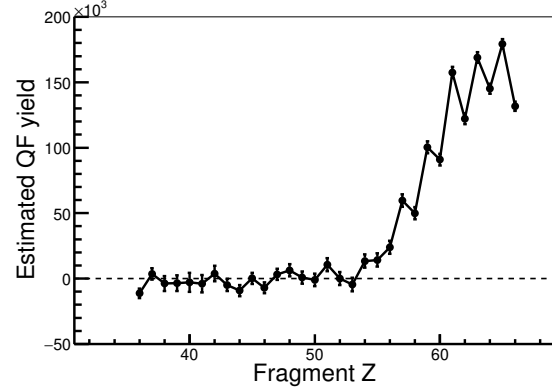


Figure 6. The figure shows the difference between the measured data and the GEF prediction of fission of the ^{265}Db CS shown in Fig. 1. The amplitude of the GEF distribution was fitted to the region between $Z=37$ and $Z=52$. The error bars show statistical and uncorrelated systematic uncertainties.

ference between the measured data and a GEF distribution of an amplitude fitted to match the region between $Z=37$ and $Z=52$. The fact that below $Z\sim 56$ the difference between both distributions randomly fluctuates around 0 is a straightforward evidence that the measured distribution below $Z\sim 56$ and the fission distribution from GEF have the same width. Therefore, the contribution of QF below $Z\sim 56$ must be negligible, in complete agreement with the indications from the mass distributions width for fixed Z , the even-odd effect, and the angular anisotropy previously discussed.

This QF contribution corresponds to between 12% and 16% of the total fission and QF production at 52.8° in c.m. The uncertainty is mostly due to the extrapolation of the remaining distribution beyond $Z=66$ and below $Z=36$, which was modelled after the data from [7, 8]. By using the angular anisotropy for fusion-fission and the measurements from [7], the total QF contribution in the full c.m. angular range can be estimated between 20% and 24%. Assuming a 100% fission probability after complete fusion,⁸ the suppression factor for the $^{238}\text{U}+^{27}\text{Al}$ channel would be between 0.76 and 0.80 (see Fig. 4). This is significantly higher than the estimation from [7] (70% of the total fission) and what the systematics of [31] suggests (a suppression factor between 0.3 and 0.5).

Concerning the systematics of [31], since the exponential decrease of the suppression factor as a function of $Z_p Z_t$ is demonstrated only for the ^{220}Th CS, one cannot help but wonder how universal is this particular behaviour. In Fig. 4, the results from [32], pertaining the formation of the ^{216}Ra , are treated to obtain the suppression factor as in [31],⁹ and shown along those of ^{220}Th and the present estimation for ^{265}Db . Despite the few and scattered points, a certain dependence on the compound system cannot be

⁸The GEF code and the PACEIV [35] program predict 97% and 100% of fission probability, respectively.

⁹The fit of the cross section as a function of the excitation energy for the $^{12}\text{C}+^{204}\text{Pb}$ reactions was obtained from the Monte Carlo statistical model calculations due to the lack of data points beyond 60 MeV.

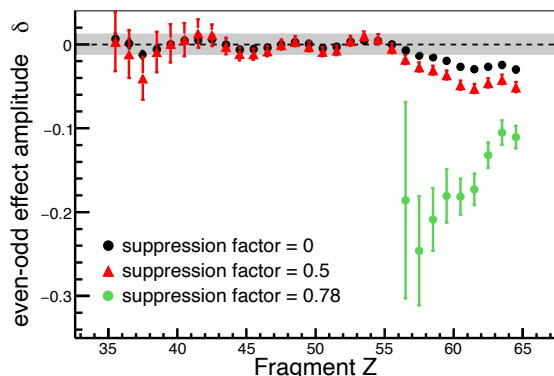


Figure 7. Even–odd effect amplitude δ as a function of Z for three different values of the suppression factor: 0 (black dots), 0.5 (red triangles), and 0.78 (green dots). The shadowed area shows the limits statistically compatible with $\delta = 0$ with a suppression factor of 0.

ruled out. Heavier compounds would seem to have suppression factors closer to 1 for a fixed $Z_p Z_t$. More data from other compound systems would be needed to confirm or refute this dependence.

As per the estimations from [7], the difference with respect to the present one might be due to the methods used, being both somehow indirect (based on assumptions on the angular anisotropy, the moments of inertia, and the Gaussian-like shape of fission distributions in [7], and on the GEF predictions of the fission fragment distribution width in this work¹⁰).

4.1 Amplitude of the even–odd effect in QF

The values of δ shown in Fig. 3 are computed with respect to the measured yields, which are indeed the sum of events corresponding to fusion–fission and quasi-fission reactions. Since δ is defined as the relative deviation to the underlying smooth distribution, the addition of events from a distribution produced with no even–odd staggering would result in an underestimation of δ that depends on the fraction of the QF yield at each Z .

Figure 7 shows δ as a function of the fragment Z in three different scenarios: a suppression factor of 0 (no fission); of 0.5 (similar to [31]); and 0.78 (as obtained in this work). Taking $Z=62$ as a reference, the amplitude of the even–odd effect ranges from $\delta = -0.03$ if no fission is considered, to $\delta = -0.05$ with a suppression factor of 0.5, and up to $\delta = -0.15$ with a factor of 0.78.

Despite this variation, some conclusions can be drawn from these δ values. The combinatorial model of proton transfer described in [26] shows that breaking any number of proton pairs in the first moments after touching produces δ amplitudes closer to 0 than the measured ones. This suggests that the initial equilibration of the proton–neutron asymmetry and the damping of the initial kinetic

energy is performed through the exchange of proton pairs, along with the unpaired proton in ^{27}Al . The δ amplitude is also compatible with a transfer probability that treats on an equal footing proton pairs and unpaired protons.

However, in order to estimate in a more quantitative way the possible effect of the transfer probability of unpaired protons and pairs, of the backflow,¹¹ and the energy dissipated in pair breaking, the actual suppression factor of $^{238}\text{U}+^{27}\text{Al}$ fusion–fission is needed.

5 Perspectives on QF studies with VAMOS

The next step after this experiment is to fully exploit the identification capabilities of VAMOS to open the doors to Z and the neutron number N as new observables in QF and bring similar breakthroughs, although in a more modest scale, as those the pioneering experiments of Schmidt et al. have brought to fission studies [36, 37].

In order to achieve this, a new experiment with VAMOS will continue the QF studies and hopefully overcome some of the difficulties of the present one [38]. The reaction to be measured is $^{186}\text{W}+^{54}\text{Cr}$ at 211 MeV in c.m. This channel was already studied in [39], where the MAD shows clear correlations associated QF with short and medium sticking times, and negligible fusion–fission contribution, thus avoiding the issues described in Sec. 4. The coverage in c.m. will also be increased: a second arm will allow 2ν coincidences to obtain the scission masses and to access forward and backward c.m. angles.

Together with the Z identification in VAMOS, the experiment will be able to produce for the first time, not only MAD, but ZAD, NAD, and NZAD, that is Z –, N –, and N/Z –angle distributions. These will allow to determine quantities like the total kinetic and excitation energies, neutron evaporation, even–odd effect, and even the scission configuration, as a function of time, and thus, track the evolution of the system along the multi-dimensional potential energy landscape.

M.C. warmly thanks the exchanges and suggestions from Prof. D. Hinde, which have prompted Sec. 4. The excellent discussions during and after the HIAS 2025 Symposium are acknowledged. This work was partially supported by the Spanish Research State Agency n° PGC2018-096717-B-C22 and PID2021-128487NB-I00, by European Union ERDF, by the "María de Maeztu" Units of Excellence program n° MDM-2016-0692, by Xunta de Galicia as Centro singular de investigación de Galicia accreditation 2019–2022, from the "Consolidación e estruturación" n° ED431F 2016/002 and ED431C 2024/13. This project has received funding from the European Union's Horizon 2020 research and innovation program under grant agreement n° 654002.

References

- [1] D.J. Hinde, M. Dasgupta, and E.C. Simpson, Experimental studies of the competition between fusion and

¹⁰Although the behaviour of δ , the angular anisotropy, and the isotopic mass distributions is also a solid indication.

¹¹That is, the probability of protons being transferred back from the light to the heavy partner.

- quasifission in the formation of heavy and superheavy nuclei. *Prog. Part. Nucl. Phys.* **118**, 103856 (2021). <https://doi.org/10.1016/j.pnpnp.2021.103856>.
- [2] E. Vardaci, M.G. Itkis, I.M. Itkis, G. Knyazheva, and E.M. Kozulin, Fission and quasifission toward the superheavy mass region. *J. Phys. G: Nucl. Part. Phys.* **46**, 103002 (2019). <http://dx.doi.org/10.1088/1361-6471/ab3118>.
- [3] C. Simenel, P. McGlynn, A.S. Umar, and K. Godbey, Comparison of fission and quasi-fission modes. *Phys. Lett. B* **822**, 136648 (2021). <https://doi.org/10.1016/j.physletb.2021.136648>.
- [4] C. Simenel, K. Godbey, and S. Umar, Timescales of Quantum Equilibration, Dissipation and Fluctuation in Nuclear Collisions. *Phys. Rev. Lett.* **124**, 212504 (2020). <https://doi.org/10.1103/PhysRevLett.124.212504>.
- [5] S. Pullanhiotan, M. Rejmund, A. Navin, W. Mittig, and S. Bhattacharyya, Performance of VAMOS for reactions near the Coulomb barrier. *Nucl. Instr. Methods A* **593**, 343 (2008). <https://doi.org/10.1016/j.nima.2008.05.003>.
- [6] M. Rejmund et al., Performance of the improved larger acceptance spectrometer: VAMOS++. *Nucl. Instr. Methods A* **646**, 184 (2011). <https://doi.org/10.1016/j.nima.2011.05.007>.
- [7] J. Töke et al., Compound Nucleus Fission and Quasi-Fission in Reactions of ^{238}U with ^{16}O and ^{27}Al . *Phys. Lett. B* **142**, 258 (1984). [https://doi.org/10.1016/0370-2693\(84\)91194-8](https://doi.org/10.1016/0370-2693(84)91194-8).
- [8] J. Töke et al., Quasi-fission – The Mass-Drift Mode in Heavy-Ion Reactions. *Nucl. Phys. A* **440**, 327 (1985). [https://doi.org/10.1016/0375-9474\(85\)90344-6](https://doi.org/10.1016/0375-9474(85)90344-6).
- [9] M. Caamaño et al., Isotopic yield distributions of transfer- and fusion-induced fission from $^{238}\text{U} + ^{12}\text{C}$ reactions in inverse kinematics. *Phys. Rev. C* **88**, 024605 (2013). <https://doi.org/10.1103/PhysRevC.88.024605>.
- [10] D. Ramos et al., Isotopic fission-fragment distributions of ^{238}U , ^{239}Np , ^{240}Pu , ^{244}Cm , and ^{250}Cf produced through inelastic scattering, transfer, and fusion reactions in inverse kinematics. *Phys. Rev. C* **97**, 054612 (2018). <https://doi.org/10.1103/PhysRevC.97.054612>.
- [11] D. Ramos et al., First Direct Measurement of Isotopic Fission-Fragment Yields of ^{239}U . *Phys. Rev. Lett.* **123**, 092503 (2019). <https://doi.org/10.1103/PhysRevLett.123.092503>.
- [12] C. Schmitt et al., Experimental Evidence for Common Driving Effects in Low-Energy Fission from Sublead to Actinides. *Phys. Rev. Lett.* **126**, 132502 (2021). <https://doi.org/10.1103/PhysRevLett.126.132502>.
- [13] C. Rodríguez-Tajes et al., Transfer reactions in inverse kinematics: An experimental approach for fission investigations. *Phys. Rev. C* **89**, 024614 (2014). <https://doi.org/10.1103/PhysRevC.89.024614>.
- [14] J. Simpson et al., The EXOGAM array: A radioactive beam gamma-ray spectrometer. *Acta Phys. Hung., New Ser. Heavy Ion Physics* **11**, 159 (2000).
- [15] S. Akkoyun et al., AGATA–Advanced GAMMA Tracking Array. *Nucl. Instr. Methods A* **668**, 26 (2012). <https://doi.org/10.1016/j.nima.2011.11.081>.
- [16] D. Fernández-Fernández, *High-energy fission and the onset of quasi-fission* (PhD at Universidade de Santiago de Compostela, 2024) <http://hdl.handle.net/10347/34202>.
- [17] K.–H. Schmidt, B. Jurado, C. Amouroux, and C. Schmitt, General Description of Fission Observables: GEF Model Code. *Nucl. Data Sheets* **131**, 107 (2016). <http://dx.doi.org/10.1016/j.nds.2015.12.009>. GEF code version 2025.1.2.
- [18] B.L. Tracy et al., Rb and Cs Isotopic Cross Sections from 40–60-MeV-Proton Fission of ^{238}U , ^{232}Th , and ^{235}U . *Phys. Rev. C* **5**, 222 (1972). <https://doi.org/10.1103/PhysRevC.5.222>.
- [19] S. Steinhäuser et al., Odd–even effects observed in the fission of nuclei with unpaired protons. *Nucl. Phys. A* **634**, 89 (1998). [https://doi.org/10.1016/S0375-9474\(98\)00148-1](https://doi.org/10.1016/S0375-9474(98)00148-1).
- [20] M. Caamaño, F. Rejmund, and K.–H. Schmidt, Evidence for the predominant influence of the asymmetry degree of freedom on the even–odd structure in fission-fragment yields. *J. Phys. G: Nucl. Part. Phys.* **38**, 035101 (2011). <https://doi.org/10.1088/0954-3899/38/3/035101>.
- [21] H. Nifenecker et al., A Combinatorial Analysis of Pair Breaking in Fission. *Z. Physik A* **308**, 39 (1982). <https://doi.org/10.1007/BF01415847>.
- [22] S. Pommé et al., Excitation energy dependence of charge odd–even effects in the fission of ^{238}U close to the fission barrier. *Nucl. Phys. A* **560**, 689 (1993). [https://doi.org/10.1016/0375-9474\(93\)90041-U](https://doi.org/10.1016/0375-9474(93)90041-U).
- [23] F. Rejmund, A.V. Ignatyuk, A.R. Junghans, and K.–H. Schmidt, Pair breaking and even–odd structure in fission-fragment yields. *Nucl. Phys. A* **678**, 215 (2000). [https://doi.org/10.1016/S0375-9474\(00\)00322-5](https://doi.org/10.1016/S0375-9474(00)00322-5).
- [24] D. Ramos et al., Experimental evidence of the effect of nuclear shells on fission dissipation and time. *Phys. Rev. C* **107**, L021601 (2023). <https://doi.org/10.1103/PhysRevC.107.L021601>.
- [25] B. Montenegro Viñas and M. Caamaño, Study of the log-third-difference method for the computation of even–odd staggering in fission yields. *Eur. Phys. J. A* **60**, 237 (2024). <https://doi.org/10.1140/epja/s10050-024-01450-z>.
- [26] M. Caamaño et al., Connection between nuclear structure, dissipation, and time in fission data. *EPJ Web of Conferences* **306**, 01020 (2024). <https://doi.org/10.1051/epjconf/202430601020>.
- [27] K.–H. Schmidt and B. Jurado, Entropy Driven Excitation Energy Sorting in Superfluid Fission Dynamics. *Phys. Rev. Lett.* **104**, 212501 (2010). <https://doi.org/10.1103/PhysRevLett.104.212501>.
- [28] B. Jurado and K.–H. Schmidt, Influence of complete energy sorting on the characteristics of the odd–even effect in fission-fragment element distributions. *J. Phys.*

- G: Nucl. Part. Phys. **42**, 055101 (2015). <https://doi.org/10.1088/0954-3899/42/5/055101>.
- [29] F. Gönnenwein, *The Nuclear Fission Process* (C. Wagemans, CRC Press, Boca Raton, FL, 1991). 409–423
- [30] L.T. Bezzina, *Examining equilibration in heavy ion fusion using precision cross section measurements* (PhD at The Australian National University, 2022) <https://doi.org/10.25911/FCPX-C451>.
- [31] L.T. Bezzina, E.C. Simpson, D.J. Hinde, and M. Dasgupta, Observation of suppression of heavy-ion fusion by slow quasifission. Nucl. Phys. A **1063**, 123198 (2025). <https://doi.org/10.1016/j.nuclphysa.2025.123198>.
- [32] A.C. Berriman, D.J. Hinde, M. Dasgupta, C.R. Morton, R.D. Butt, and J. O. Newton, Unexpected inhibition of fusion in nucleus–nucleus collisions. Nature **413**, 144 (2001). <https://doi.org/10.1038/35093069>.
- [33] D. Ramos et al., Insight into excitation energy and structure effects in fission from isotopic information in fission yields. Phys. Rev. C **99**, 024615 (2019). <https://doi.org/10.1103/PhysRevC.99.024615>.
- [34] D. Ramos, *Fragment Distributions of Transfer- and Fusion-Induced Fission from $^{238}\text{U}+^{12}\text{C}$ Reactions Measured Through Inverse Kinematics* (PhD at Universidade de Santiago de Compostela, 2016) <https://hdl.handle.net/10347/15070>.
- [35] O.B. Tarasov and D. Bazin, LISE++: Radioactive beam production with in-flight separators. Nucl. Instr. Methods B **266**, 4657 (2008). <https://doi.org/10.1016/j.nimb.2008.05.110>. PACEIV code version 4.34.14.
- [36] K.-H. Schmidt et al., Relativistic radioactive beams: A new access to nuclear-fission studies. Nucl. Phys. A **665**, 221 (2000). [https://doi.org/10.1016/S0375-9474\(99\)00384-X](https://doi.org/10.1016/S0375-9474(99)00384-X).
- [37] C. Böckstiegel et al., Nuclear-fission studies with relativistic secondary beams: Analysis of fission channels. Nucl. Phys. A **802**, 12 (2008). <https://doi.org/10.1016/j.nuclphysa.2008.01.012>.
- [38] C. Schmitt and M. Caamaño, *Novel insight into quasi-fission for advancing the understanding of reaction dynamics* (Exp. E900_24, GANIL PAC November 2024).
- [39] K. Hammerton et al., Reduced quasifission competition in fusion reactions forming neutron-rich heavy elements. Phys. Rev. C **91**, 041602(R) (2015). <https://doi.org/10.1103/PhysRevC.91.041602>.